JGR Atmospheres

RESEARCH ARTICLE
10.1029/2021JD036130

Key Points:

- A Terrestrial Gamma-ray Flash (TGF) occurring in a not previously reported context has been observed at ground level at the Lightning Observatory in Gainesville
- The TGF had a duration of 35 μs and was inferred to be produced by a negative leader in a decayed channel of the preceding positive stroke
- To date, five TGFs were recorded at ground level in Florida and none of them was associated with the lightning flash initiation process

Correspondence to:
I. Kereszy,
ikereszy@ufl.edu

Citation:
Kereszy, I., Rakov, V. A., Ding, Z., & Dwyer, J. R. (2022). Ground-based observation of a TGF occurring between opposite polarity strokes of a bipolar cloud-to-ground lightning flash. *Journal of Geophysical Research: Atmospheres*, *127*, e2021JD036130. https://doi.org/10.1029/2021JD036130

Received 31 OCT 2021
Accepted 10 APR 2022

Ground-Based Observation of a TGF Occurring Between Opposite Polarity Strokes of a Bipolar Cloud-To-Ground Lightning Flash

I. Kereszy[1,2], V. A. Rakov[1], Z. Ding[1], and J. R. Dwyer[3]

[1]Department of Electrical and Computer Engineering, University of Florida, Gainesville, FL, USA, [2]Department of Physics, University of Florida, Gainesville, FL, USA, [3]Department of Physics and Astronomy, University of New Hampshire, Durham, NH, USA

Abstract We present the ground-based observation of a terrestrial gamma-ray flash (TGF) that occurred between positive (second) and negative (third) strokes of a five-stroke bipolar cloud-to-ground lightning flash. Those two strokes shared the same channel to ground at a distance of 200 m or so from the Lightning Observatory in Gainesville (LOG), Florida. Earlier TGF observations at ground level in Florida (a total of four) were either associated with the initial continuous current (ICC) of rocket-triggered lightning flashes or occurred during the relatively steady current following the return-stroke current peak in natural lightning flashes; that is, in the presence of current-carrying channel to ground. The TGF presented here occurred in a different context: at the early (in-cloud) stage of negative leader entering the remnants of the channel previously created by the positive stroke. The TGF had a duration of 35 μs and consisted of 18 pulses with amplitudes ranging from 114 to 912 keV. The overall flash context in which the TGF occurred was as follows. The first (143-kA) stroke was negative and terminated on ground 1.4 km from LOG, the second (12-kA) stroke was positive and forged a new path to ground about 200 m from LOG, and the third (28-kA) stroke (TGF producer) was negative and followed the path of the second (positive) stroke. The fourth (43-kA) stroke was negative and created a new termination on ground about 900 m from LOG, and the fifth (4.5-kA) stroke was also negative and followed the fourth-stroke channel.

Plain Language Summary Thunderstorms are known to produce bursts of energetic radiation called Terrestrial Gamma-ray Flashes, but they are usually observed from satellites and very rarely from the ground. Here we present one of these rare observations, which was made during a bipolar lightning flash. This is a new context for TGF production that hasn't been reported before. The TGF was recorded at the Lightning Observatory in Gainesville (LOG), Florida, on 2 November 2018 at the early (in-cloud) stage of negative leader entering the remnants of the channel previously created by the positive stroke. The TGF had a duration of 35 μs and consisted of 18 pulses with amplitudes ranging from 114 to 912 keV.

1. Introduction

Terrestrial Gamma-ray Flashes (TGFs) are defined here as bursts of gamma-rays less than 1 ms or so in duration, whose sources are located inside thunderclouds, at altitudes of several kilometers or more above the ground level. In contrast, X-rays/gamma-rays (in lightning research, the boundary between the two is usually placed at 1 MeV) are produced by all types of downward leaders when they come typically within 100 m or so of the ground (e.g., Dwyer et al., 2004a; Mallick et al., 2012). In either case, avalanches of runaway electrons experiencing deflection by the electric field of other charged particles (typically atomic nuclei) are involved. However, specific mechanisms/scenarios may differ, depending on the source of seed electrons, magnitude and spatial extent of electric field, and other factors. Energetic radiation associated with downward leaders in negative cloud-to-ground flashes (-CGs) is usually detected (and identified as such) within less than 1 ms of the return-stroke onset (see, e.g., Figure 7 of Mallick et al. (2012)). TGFs are mostly observed from space (e.g., Briggs et al., 2010; Fishman et al., 1994; Neubert et al., 2020; Smith et al., 2005) and rarely seen at the ground. The previous ground-based observations are reviewed next.

Tran et al. (2015) reported on a TGF observed in 2014 at the Lightning Observatory in Gainesville (LOG), Florida. It was associated with a single-stroke 224-kA -CG at a distance of 7.5 km from LOG. The TGF had a duration of 16 μs and was composed of 6 detectable photons, four of which were in the MeV-range. The corresponding RF

Table 1
Summary of Ground-Level Observations of Terrestrial Gamma-Ray Flashes (TGFs)

Reference	Dwyer et al. (2004b)	Dwyer et al. (2012)	Tran et al. (2015)	Hare et al. (2016)	Belz et al.[c] (2020)	Present study
Location	Camp Blanding, Florida	Camp Blanding, Florida	LOG, Florida	Camp Blanding, Florida	Telescope Array Surface Detector (TASD), Utah	LOG, Florida
Date	15 August 2003	30 June 2009	13 June 2014	15 August 2014	2 August 2018	2 November 2018
Distance from ground-termination point (km)	0.65	about 1.1	7.5	Within hundreds of meters	Within a few kilometers	about 0.2
Type of lightning	Rocket-triggered (classical) negative flash	Natural negative flash	Natural negative flash	Rocket-triggered (altitude) negative flash	Natural negative flash	Natural bipolar flash
Number of Return Strokes	NA	1	1	2 (including quasi-RS of altitude triggered flash)	1 or more	5
TGF context	During ICC pulse	After return stroke	After return stroke, accompanied by dE/dt burst	During ICC pulse	During Initial Breakdown Pulse (IBP)	At the beginning of third (negative) leader
Peak Current (kA)	11 (ICC pulse)	99 (RS)	224 (RS)	14 (ICC pulse)	37 (IBP)	28 (third RS)
TGF starting time	40 ms after start of initial stage	191 μs after return stroke onset	202 μs after return stroke onset	13 ms after quasi-RS of altitude triggered flash	~1 ms after flash initiation	1.1 ms before (third) return stroke onset
Number of photons	227	19	6	System saturated after 50 μs	NA	18
TGF duration (μs)	300	53	16	290	10	35
Photon energy	up to 11 MeV	64 keV to >20 MeV[a]	95 keV to >13 MeV[a]	Several MeVs and more (system saturated)	Several MeVs (inferred)	114–912 keV
Multiple X-rays/ gamma-rays during leader stage	NA	Yes	No[b]	NA	NA	Yes (at the end of leader stage)

[a]The largest X-ray/gamma-ray pulses in 2009 and 2014 were saturated at 5–6 MeV. Their amplitudes were estimated via reconstruction described by Dwyer et al. (2012). [b]A single pulse (930 keV) occurred 1.34 ms before the return stroke. [c]Only the strongest TGF in the event which is labeled TGF A and described in detail in the paper. TASD is a large area (700 km^2) array of 507 scintillator detectors (1.2 km^2 square-gridding size) designed for the detection of cosmic ray showers, located 1.4 km above sea level.

electromagnetic field signatures were recorded at LOG and supplemented by field signatures at larger distances recorded by the U.S. National Lightning Detection Network (NLDN) and the Earth Networks Total Lightning Network (ENTLN). The TGF occurred 202 μs after the return-stroke onset and was accompanied by an electric field derivative (dE/dt) burst. The latter observation suggests that RREA or other relativistic process responsible for the TGF production and the low-energy streamer formation process responsible for the dE/dt burst can be taking place concurrently. Other ground-based TGF observations in Florida include three events recorded at Camp Blanding, two associated with rocket-and-wire triggered lightning (Dwyer et al., 2004b; Hare et al., 2016) and one with natural lightning (Dwyer et al., 2012). All four previously reported events from Florida occurred in the presence of steady current carrying negative charge to ground, well after the flash initiation processes. In contrast, Belz et al. (2020) reported TGFs associated with the initial (preliminary) breakdown or first-leader process from recent ground-based observations in Utah. NLDN-reported peak currents, inferred from the RF field signatures of the initial breakdown, were a few tens of kiloamperes. TGFs occurring in a similar context, but in association with larger-amplitude (>100 kA) IC pulses were also observed at ground level during winter thunderstorms in Japan by Wada, Enoto, Nakamura et al. (2019), (2020) and Hisadomi et al. (2021). All ground-based observations of TGFs in Florida and Utah published to date are summarized in Table 1. The Japanese

observations are not included in the Table due to the lack of specific information on the TGF duration. The context of the two TGFs presented by Wada, Enoto, Nakamura et al. (2019), (2020) and one TGF presented by Hisadomi et al. (2021) was described by the authors as gamma-ray glows (typical duration of the order of minutes) terminated by a lightning discharge producing a wideband RF electromagnetic field signature referred to as "negative energetic intracloud pulse" or -EIP associated with negative charge moving downward (the term EIP was introduced by Lyu et al. (2015)). The magnitudes of the associated peak currents were estimated to be 260 and 197 kA in Wada et al. (2020) and 122 kA in Hisadomi et al. (2021). Termination of gamma-ray glows (also referred to as Thunderstorm Ground Enhancements or TGEs) was previously observed by Chilingarian et al. (2017), (2020).

There is presently no consensus on the nature of EIPs: Tilles et al. (2020) have suggested that the EIP is produced by the current of relativistic electron avalanches (by the current of the TGF itself, without any hot channel involved), while Østgaard et al. (2021) have argued (based on the associated red emission detected from space) that EIPs do involve hot channels. Lyu and Cummer (2018) reported on 23 -EIPs, 18 of which were labeled by them as "PB-type or early -EIPs", and 5 as "PreRS-type or late -EIPs". They conjectured that -EIPs "may be signatures of downward TGFs." We did not find any evidence of PB-type -EIPs (pulses with durations of a few tens of microseconds and NLDN-reported currents >100kA) in the present study. In fact, the NLDN did not report any event associated with our TGF, and the ENTLN reported an intracloud (IC) event with an estimated peak current of 7.5 kA. Individual ENTLN electric field waveforms are not shown here because, partly due to the memory-saving processing, they are highly irregular and differ significantly from station to station with no field signature at all in the record corresponding to the closest (24 km) station.

Distances between TGFs and detectors in the various ground-level observations (Abbasi et al., 2018; Belz et al., 2020; Dwyer et al., 2004b; Hare et al., 2016; Wada, Enoto, Nakamura, et al., 2019, Wada, Enoto, Nakazawa, et al., 2019) were estimated to be some kilometers or less versus 600 km or more in satellite observations. It is possible that some lower-intensity TGFs occurring not far from the cloud base can be detected at the ground level, but not from orbit.

In this paper, we present a TGF occurring in a not previously reported context, between opposite polarity strokes of a bipolar cloud-to-ground lightning flash. Bipolar lightning discharges sequentially transfer to ground both positive and negative charges during the same flash (Rakov, 2005). They constitute about 10% of the global lightning activity. High-speed optical images of bipolar flashes in which a negative downward leader developed in the channel to ground previously created by a positive stroke were reported by Saba et al. (2013) and Saraiva et al. (2014). The TGF presented here was recorded at LOG with the same instrumentation as the TGF reported by Tran et al. (2015). The possible role of decayed (i.e., non-luminous and carrying essentially no current; see, e.g., Rakov & Uman, 2003, Section 4.7.8), but still warm lightning channels inside the cloud in generation of TGFs occurring well after the flash-initiation process is discussed. It is worth noting that the role of the remnants of previously created channel in making subsequent-stroke leaders near ground more prolific X-ray/gamma-ray producers than their corresponding first-stroke leaders was discussed by Mallick et al. (2012) and Tran et al. (2019).

2. Experimental Setup

The electric field (E), magnetic field derivative (dB/dt), and X-ray/gamma-ray data presented in this paper were obtained at the Lightning Observatory in Gainesville (LOG), Florida, which is located on the roof of the five-story New Engineering Building (NEB) on the University of Florida campus. The E-field measurement system used a 0.155 m^2 flush-mounted flat-plate antenna followed by a unity gain, high-input-impedance amplifier with an active integrator. The E-field enhancement factor due to the presence of NEB was estimated to be 1.4 (Baba & Rakov, 2007). The E-field measuring system (one of the two, with a lower gain) had a useful frequency bandwidth of 16 Hz to 10 MHz, with a decay time constant of 10 ms. The output signal was transmitted through an Opticomm fiber-optic link to the LeCroy HRO 64Zi digitizing oscilloscope which sampled at 100 MHz. The dB/dt antenna was a vertical loop with an area of 0.533 m^2. Its plane was oriented in the east-west direction. The dB/dt measuring system had a −3 dB upper frequency response of 16 MHz. The E and dB/dt records were used to identify different lightning processes, determine the return-stroke onset times, and estimate leader durations.

Table 2
Summary of NLDN-Reported Data for Five Strokes Whose Locations are Shown in Figure 1

Event ID	Time (UTC)	Distance from LOG (km)	Peak current (kA)	Interstroke interval (ms)	Latitude (degrees N)	Longitude (degrees W)	Number of reporting stations	Remarks
Stroke 1	19:40:49.578	1.41	−143	NA	29.633	−82.336	29	Negative
Stroke 2	19:40:49.590	0.26	12	12	29.640	−82.348	4	Positive, new ground termination
Stroke 3	19:40:49.601	0.14	−28	11	29.642	−82.3460	25	Negative, TGF producer
Stroke 4	19:40:49.629	0.70	−43	28	29.647	−82.342	26	Negative, new ground termination
Stroke 5	19:40:49.651	1.09	−4.5	22	29.648	−82.338	3	Negative

X-rays/gamma-rays were recorded by the same instrument as was used by Mallick et al. (2012) and Tran et al. (2015), (2019). It consists of a NaI(Tl) scintillator of cylindrical shape with both its height and diameter equal to 7.6 cm coupled to a photomultiplier tube (PMT) and associated electronics. The detector was powered by a 12 V battery and housed in an aluminum box with a wall thickness of 0.32 cm that shielded it from electromagnetic coupling, moisture, and light, but allowed photons with energies down to 30 keV to enter. The X-ray/gamma-ray detector's output signal was transmitted through an Opticomm fiber-optic link to the LeCroy HRO 64Zi digitizing oscilloscope which sampled at 100 MHz. The 662 keV photons emitted by a radioactive source (Cs-137) were used to calibrate the detector. The upper and lower measurement limits of the detector (determined by the voltage range of the fiber-optic link and the noise level) were 5.7 MeV and 75 keV, respectively.

Using this same X-ray/gamma-ray detector installed at the same location (LOG), Mallick et al. (2012) estimated the occurrence of detectable background (not lightning related) X-rays/gamma-rays to be 1 in 8 ms. The probability that the observed X-ray/gamma-ray emissions are non-lightning-related can be estimated using the Poisson distribution (e.g., McClave & Dietrich, 1979, pp. 143):

$$P(k) = \frac{e^{-\lambda}\lambda^{k}}{k!},$$

where λ is the average number of background X-ray/gamma-ray pulses in a given time interval and k is the observed number of X-ray/gamma-ray pulses in that interval. Mallick et al. (2012) attributed X-ray/gamma-ray pulses to first or subsequent leader near ground if the X-ray/gamma-ray emission occurred within 2 ms prior to the corresponding return-stroke onset. With the observed background rate of X-ray/gamma-ray pulse occurrence (0.25 in a 2 ms interval), the probabilities that 1, 2, or 3 pulses occurred within 2 ms due to background are 0.194, 0.024, and 0.002, respectively. For four or more pulses this probability is <0.0001 (vanishingly small; Mallick et al. (2012) observed up to 109 X-ray/gamma-ray pulses associated with a single leader).

3. Data Presentation and Analysis

3.1. General Overview of TGF-Producing Flash

We present here a terrestrial gamma-ray flash that occurred between positive (second) and negative (third) strokes of a five-stroke bipolar cloud-to-ground lightning flash. Those two strokes shared the same channel to ground at a distance of 200 m or so from the Lightning Observatory in Gainesville (LOG), Florida. The flash occurred during an active thunderstorm over Gainesville, Florida, that was moving to north-east. Radar reflectivity values within a few kilometers of LOG were 40–45 dBZ. The upper cloud boundary extended to an altitude of 10 km or so.

A map showing NLDN-reported locations (locations determined based on the NLDN data; see Table 2) for all five strokes and eight preliminary breakdown (PB) pulses, along with the corresponding 50% location error ellipses is presented in Figure 1. The 50% location error ellipse is reported by the NLDN for each stroke location and defined as confidence region for which there is 50% probability that the actual stroke location lies within the area circumscribed by the ellipse, with the center of the ellipse being the most probable (reported) stroke location. Overlapping location error ellipses are often viewed as evidence that the strokes developed in the same channel to ground. Thus, it is likely that the flash in question created a total of three channels to ground, the first one taken

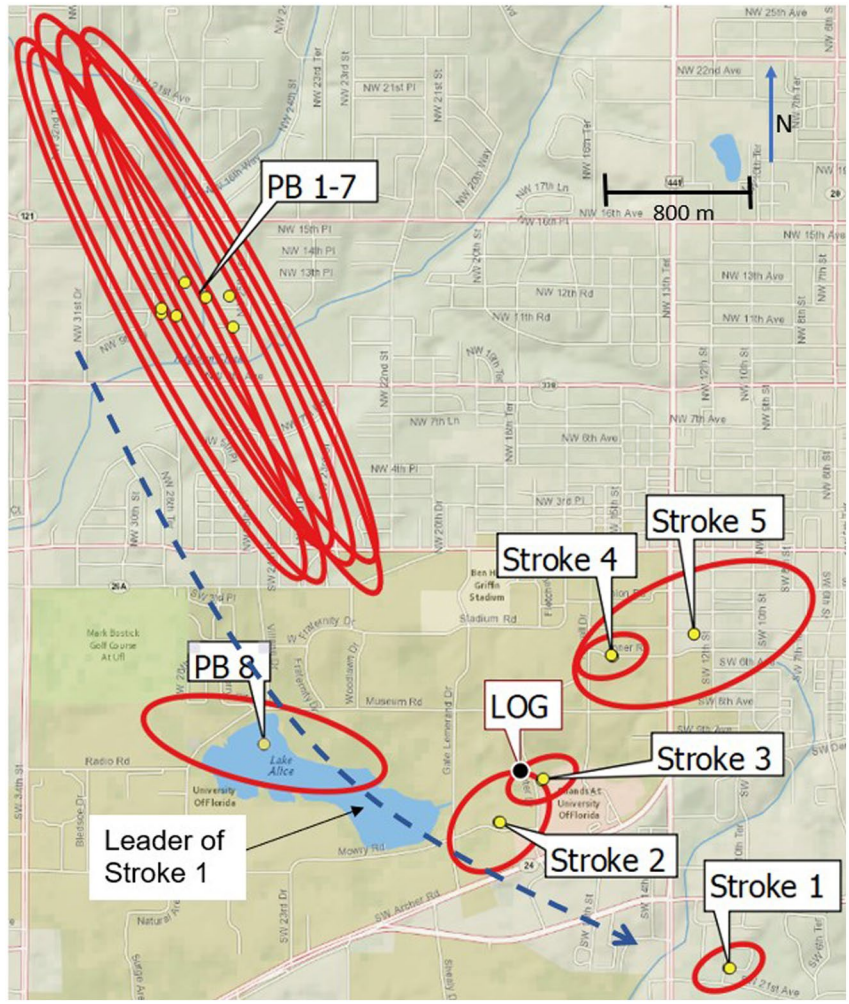

Figure 1. National Lightning Detection Network (NLDN)-reported locations (small yellow circles) of five lightning strokes and eight preliminary breakdown (PB) pulses of bipolar flash during which the Terrestrial Gamma-ray Flash (TGF) presented in this paper was observed. The location of Lightning Observatory in Gainesville is shown by a larger black circle. NLDN-reported 50% location error ellipses are shown in red. Blue broken-line arrow shows an approximate horizontal path that the leader of Stroke 1 had to follow from the PB location to the ground termination point. Strokes 1, 3, 4, and 5 were negative, and Stroke 2 was positive. The TGF was produced during the early leader stage of Stroke 3.

by Stroke 1 only, the second one taken by Strokes 2 and 3, and the third one by Strokes 4 and 5. Seven out of the eight PB pulses occurred (in plan view) very close to each other.

The overall E-field, dB/dt, and X-ray/gamma-ray records of the flash are shown in Figure 2. In showing E-field records throughout this paper, we use the atmospheric electricity sign convention (e.g., Rakov & Uman, 2003, Section 1.4.2), according to which the downward directed electric field or electric field change vector is assumed to be positive. No optical records were obtained because all the three channels to ground (see Figure 1 and associated text above) were outside the fields of view of the high-speed framing cameras installed at LOG (they were all facing west).

3.2. Preliminary Breakdown and Stroke 1 (Negative)

Data for the preliminary (initial) breakdown followed by the first leader/return stroke sequence are shown in Figure 3. Electric field and dB/dt pulses associated with the preliminary breakdown (PB) are shown in Figure 4. The PB is identified by a sequence of nine detectable electric field pulses, occurring within a typical PB time interval of 1 ms or so at the very beginning of the flash (see Figures 3a and 3b and Figures 4a and 4b).

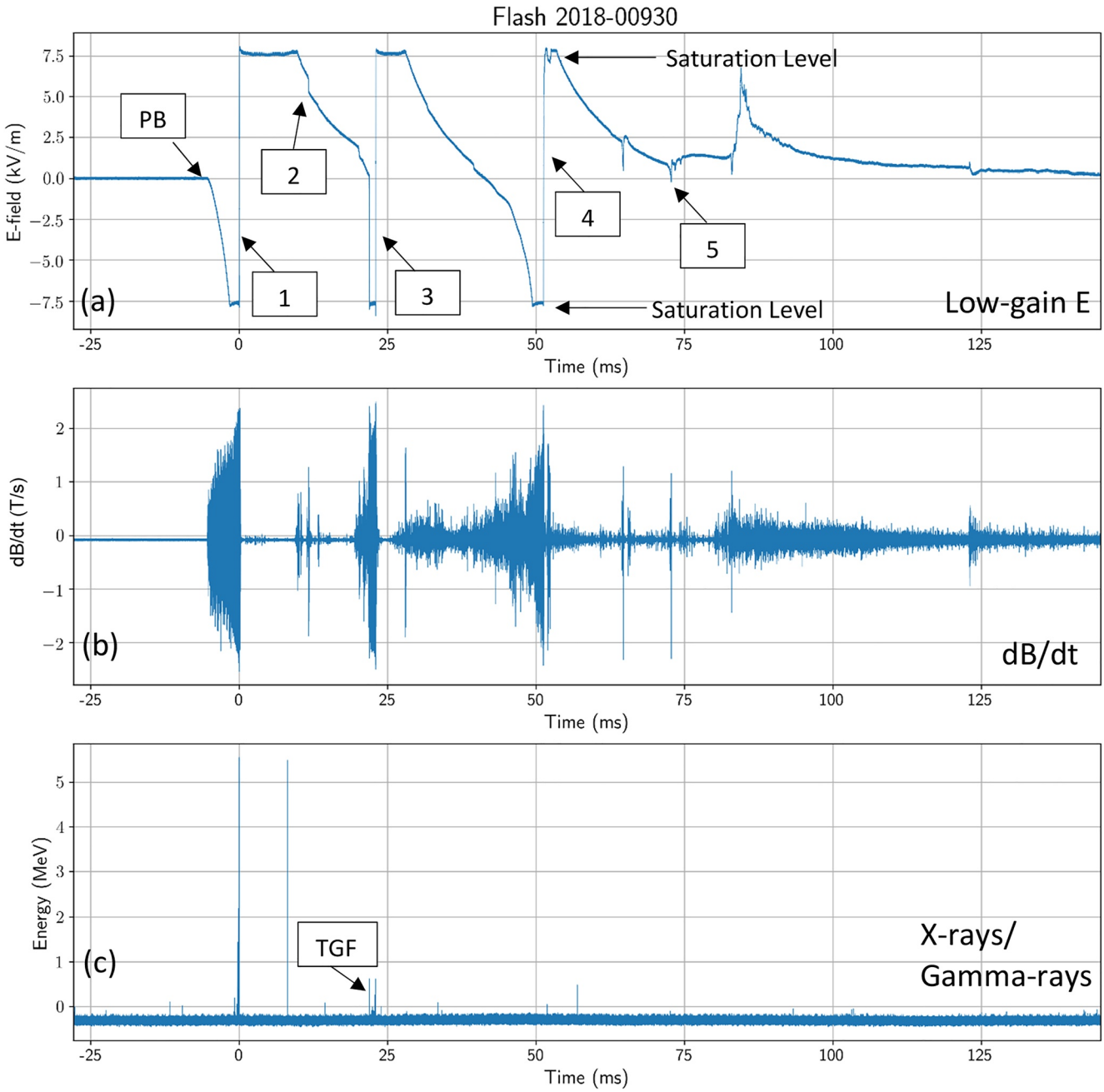

Figure 2. Overall records of (a) low-gain electric field ($\tau = 10$ ms), (b) magnetic field derivative (dB/dt), and (c) X-rays/gamma-rays for the five-stroke bipolar flash during which the Terrestrial Gamma-ray Flash presented in this paper was observed. In (a), preliminary breakdown (PB) stands for the preliminary (initial) breakdown and the numbers indicate stroke order. Electric field and dB/dt records for Strokes 1, 3, and 4 are clipped due to saturation of the measuring systems. Full time scale is 175 ms. Time t = 0 corresponds to the onset of the return-stroke stage of Stroke 1.

We present the PB signatures here because in other studies (e.g., Belz et al., 2020) TGFs were found to be associated with PB pulses. In this study, there were no detectable X-ray/gamma-ray pulses during the PB process (see Figure 3c). As seen in Figure 1, seven of the eight PB pulses were geolocated as a tight cluster to the northwest from LOG, at distances ranging from 2.45 to 2.76 km. The eighth pulse was located more or less to the west of LOG at a distance of 1.30 km. The leader of Stroke 1 attached to the ground to the south-east of LOG, at a distance of 1.41 km from it (see Figure 1), so that it had to propagate about 4 km horizontally from the PB

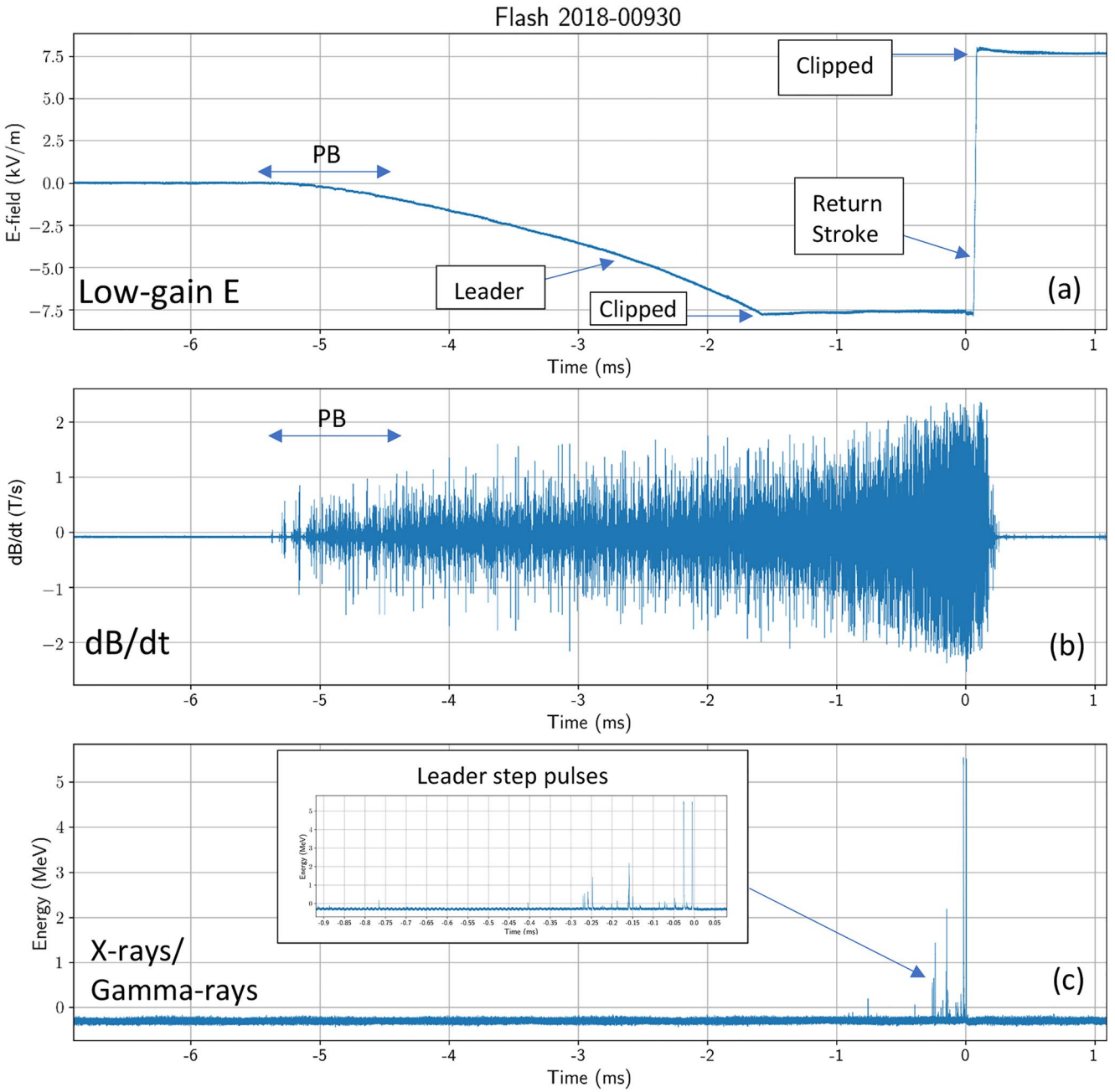

Figure 3. Same as Figure 2, but for the preliminary breakdown (PB) and Stroke 1. Time t = 0 corresponds to the onset of the return-stroke stage of Stroke 1, as determined from the dB/dt record. The stepped leader of Stroke 1 produced X-rays/gamma-rays (some exceeding the 5-MeV level) within 1 ms of the return-stroke onset. Full time scale is 8 ms. PB is shown on an expanded time scale in Figure 4.

location (PB 1-7) to the ground termination point (labeled Stroke 1), with that propagation path being over or very close to the LOG.

The leader of Stroke 1 had duration of 4–5 ms (see Figures 3a and 3b), which is considerably shorter than the typical stepped-leader duration of 35 ms (see Fig. 4.14a of Rakov & Uman, 2003). The reason for this is the unusually high intensity of Stroke 1: the NLDN-reported peak current is 143 versus 30 kA typically observed for first strokes in negative lightning. According to Zhu et al. (2016), high-intensity strokes are characterized, besides shorter leader durations (and by inference higher speeds), also by a higher intensity of PB radiation field pulses. In our electric field record, PB pulse signatures are dominated by the electrostatic and induction components,

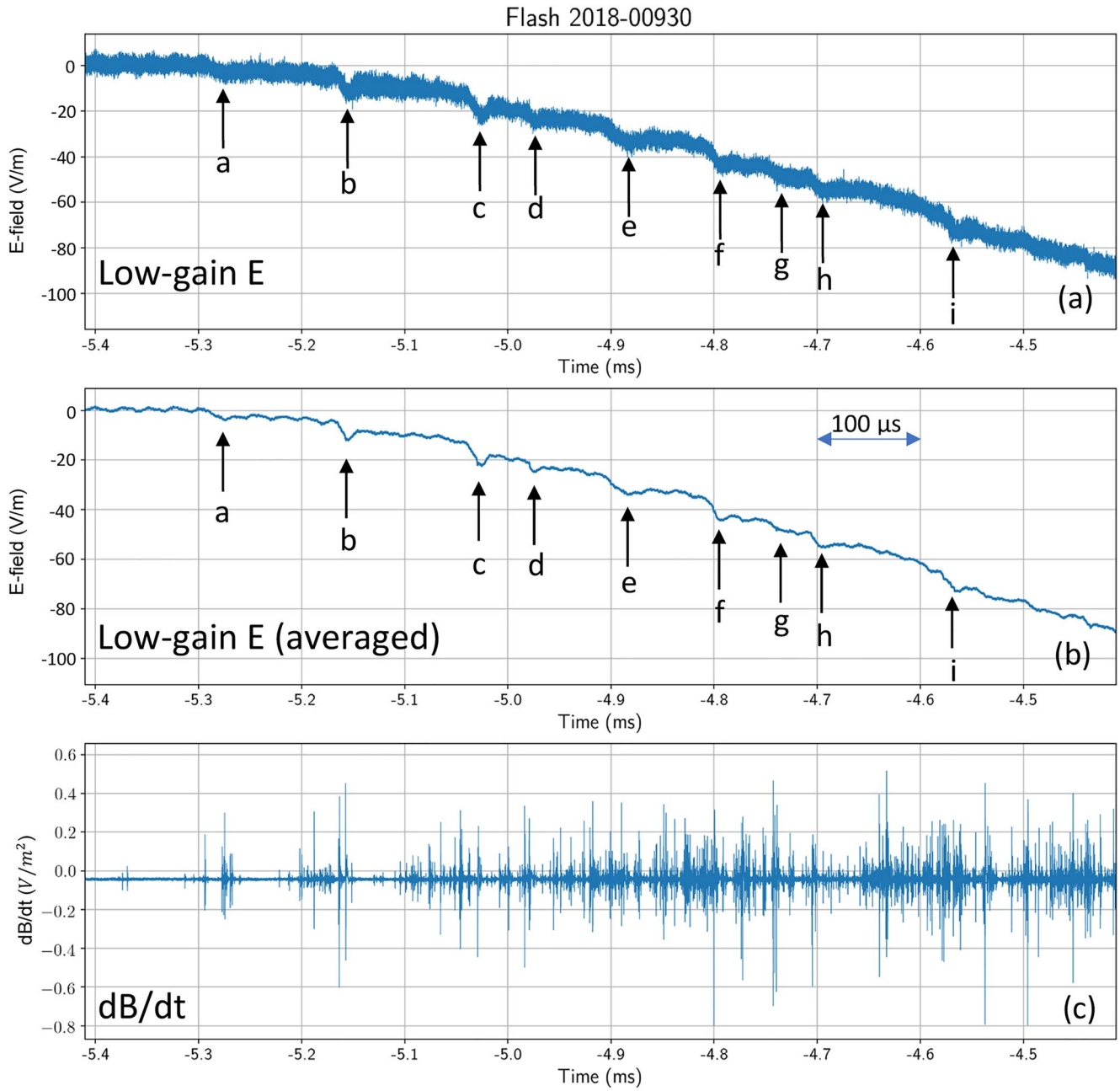

Figure 4. Preliminary breakdown as seen in (a) raw electric field, (b) 100-point moving-window time-averaged electric field, and (c) dB/dt records. Upward arrows in (a) and (b) indicate nine discernible preliminary breakdown (PB) pulses. The time intervals between the PB pulses labeled "a" through "i" in (a) and (b) are 118, 129, 54, 95, 90, 73, 22, and 132 µs. National Lightning Detection Network (NLDN) recorded eight out of the nine PB pulses (missed the pulse labeled "c"). Note that the pulses (ripples) seen in (a and b) are recorded at <3 km and, hence, are essentially electrostatic/induction, while the NLDN recorded the corresponding radiation pulses (at distances of tens to hundreds of kilometers, since the average NLDN baseline is about 350 km). The NLDN-reported polarity of radiation pulses is opposite to that of the electrostatic/induction pulses and is the same as the polarity of the return-stroke waveform (see Figure 3a), as expected. No X-rays/gamma-rays were detected during the PB process.

with the radiation field peaks being indiscernible, which is expected at distances of a few kilometers or less (see, e.g., Figure 9 of Nag & Rakov, 2016). Based on the high peak current value for Stroke 1, it is reasonable to assume that the PB intensity was also high, but still it did not produce detectable X-ray/gamma-ray pulses at LOG (see Figure 3c). The leader of Stroke 1 did produce X-ray/gamma-ray pulses (see Figure 3c, including the inset). Those pulses are associated with leader stepping near ground and are not further discussed in this paper.

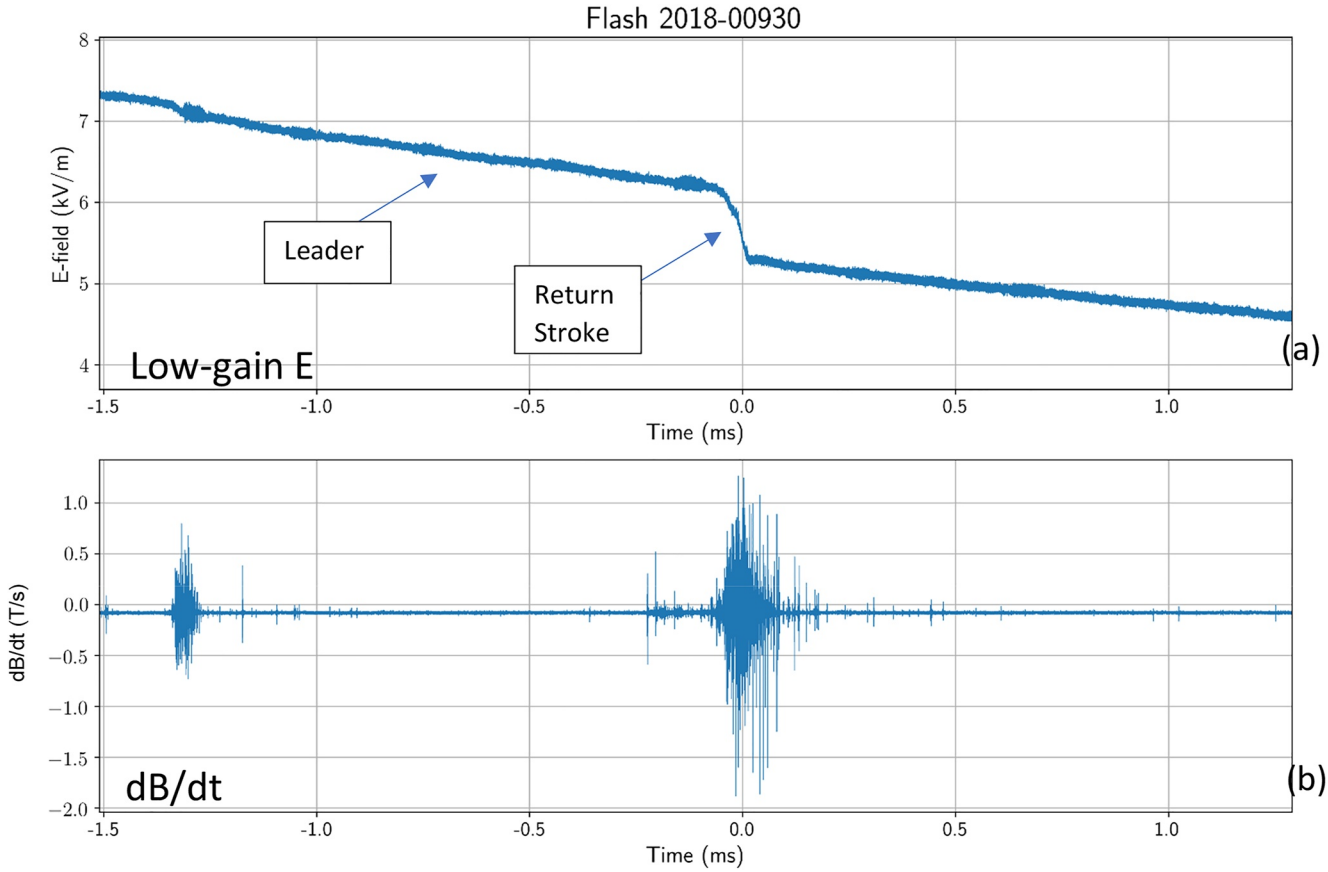

Figure 5. (a) Electric field and (b) dB/dt waveforms of Stroke 2 (positive). Time t = 0 corresponds to the onset of the return stroke stage of Stroke 2. Full time scale is 3 ms.

3.3. Stroke 2 (Positive)

Electric field and dB/dt signatures of Stroke 2 (positive) are shown in Figure 5. This stroke was reported by the NLDN as positive CG, and its polarity is confirmed by the polarity of the associated electric field change seen in Figure 5a, which is opposite to the polarity of electric field changes of the negative return strokes in the same flash (see, e.g., Figure 3a). The NLDN-reported peak current was relatively small (12 kA), but still Stroke 2 forged a new path to ground and terminated about 200 m from LOG. Since Strokes 2 and 3 developed in the same channel, we assigned the same (average) distance to both of them (the NLDN-reported distances are 0.26 and 0.14 km, respectively).

As noted in Section 3.2, the leader of Stroke 1 had to propagate from the PB location, passing over LOG, to the ground termination point, about 4 km horizontally from the PB location (see Figure 1). The approximate path of the leader of Stroke 1 from the PB location to the ground termination point of Stroke 1 is shown in Figure 1 by a broken-line arrow. This means that the return stroke (RS) of Stroke 1 (negative) moved positive charge essentially over the LOG to the PB location, injecting that positive charge into the negative leader corona sheath and discharging negative leader branches. It is conceivable that one of those branches could become positively charged, lose connection with the main channel, extend toward the ground, and manage to produce a relatively small positive RS near LOG, as reported by the NLDN. This "non-classical" scenario leading to the production of positive RS could be the reason for the shape of the leader/RS electric field signature for Stroke 2 being different from its counterparts for other strokes in this flash. Specifically, the hook-shaped leader waveform expected at close distances is missing in Stroke 2 (a feature that we did occasionally observe in electric field records of other +CGs with optically imaged channels to ground).

Note that Stroke 2 occurred at a distance of about 200 m from LOG and, hence, its electric field waveform is dominated by the electrostatic component (the radiation field peak is indiscernible, even in the integrated dB/dt waveform).

No X-rays/gamma-rays were detected from Stroke 2.

3.4. Stroke 3 (Negative, TGF Producer)

Data for Stroke 3 are shown in Figures 6 and 7. As noted above, we inferred that Stroke 3 followed the remnants of the channel to ground formed by Stroke 2. This is confirmed (besides their overlapping location error ellipses; see Figure 1) by the <3 ms duration of the leader of Stroke 3 (see Figure 6), which is characteristic of a leader developing in a previously created channel (leaders creating a new channel usually take tens of milliseconds to reach ground). In our opinion, it is likely that the leader of Stroke 3 started in the vicinity and beyond of the PB location (the flash origin) and extended south-east along the remnants of the channel of Stroke 1, toward the ground-termination point of the latter (see Figure 1), but was intercepted by the less-decayed channel of Stroke 2 near LOG.

Subsequent-stroke leaders near ground are known to produce detectable X-ray pulses, which was first unambiguously shown during rocket-triggered lightning experiments (Dwyer et al., 2003). The leader of Stroke 3 produced 15 X-ray pulses (marked in Figure 6c), which is expected given a small distance (about 200 m) from the detector and a relatively high, for a subsequent stroke, NLDN-reported peak current of 28 kA (see Table 2). What was novel is a burst of energetic radiation (TGF) that occurred at the early stage of the leader process (see Figures 6c and 7b). The TGF occurred at the time when the leader electric field change exhibited an abrupt downward deflection (around −1.2 ms; see Figure 6a), which is probably indicative of the in-cloud leader (developing predominantly horizontally between roughly −3 and −1.2 ms; see Figure 6a) abruptly turning toward ground, presumably due to interception of that leader by a less-decayed residual channel of Stroke 2. Similar to the TGF presented by Tran et al. (2015), there is a significant intensification in the field-derivative signal at the time of the TGF presented here (see Figures 6b and 6c). There are, however, some differences. In the previously reported event, the dE/dt burst is localized, while in the present case the dB/dt signal remains elevated after the TGF, through the return-stroke onset, and it is preceded by two smaller dB/dt bursts, not accompanied by detectable X-rays/gamma-rays.

To summarize, we speculate that the negative leader initiating Stroke 3, while developing inside the cloud along the residual channel of Stroke 1, entered the remnants of the warmer channel to ground created by Stroke 2 (the time elapsed since the RS of Stroke 2 was as short as 10 ms vs. 22 ms elapsed since the RS of Stroke 1; see Table 2), where the friction curve should be lower than in the channel of Stroke 1 (or in cold air), as further discussed in Section 4.

Typical dart or dart-stepped leaders initiating subsequent return strokes propagate at speeds of the order of 10^6–10^7 m/s (e.g., Rakov & Uman, 2003, Ch. 4). The leader duration corresponding to its predominantly vertical extension in Figure 6 appears to be of the order of 1 ms, which means that it traversed a channel whose length probably was 1–10 km, depending on leader speed (not available in this study). Since the cloud base in Florida is typically at an altitude of 1–1.5 km, it is likely that the leader of Stroke 3 was still inside the cloud when the TGF was generated. Later, this leader produced X-ray pulses characteristic of the stepping process, which implies that it was a dart-stepped leader (although dart leaders are also known to produce X-rays as they approach the ground). The pattern of the X-ray-pulse sequence associated with leader stepping near ground was very different from that of the TGF. Specifically, the 15 leader-step pulses that occurred over about 700 μs were separated by time intervals ranging from 6.6 to 177 μs (mean = 47 μs) and tended to increase in amplitude as the leader was approaching the ground (moving into the increasing electric field region; see Figure 3 of Nag & Rakov, 2016). In contrast, the TGF was a compact (35 μs) burst with interpulse intervals ranging from 0.9 to 7.7 μs (mean = 1.9 μs) and pulse amplitudes showing an increasing trend followed by an irregular variation. This a factor of 25 disparity in interpulse intervals, along with the different overall pulse sequence pattern, suggests that the TGF was associated with a process other than leader stepping. We hypothesize that the TGF seen in Figures 6c and 7b resulted from the negative in-cloud leader entering the upper part of a warmer channel to ground created by the preceding stroke and encountering a relatively sharp air-density gradient (probably

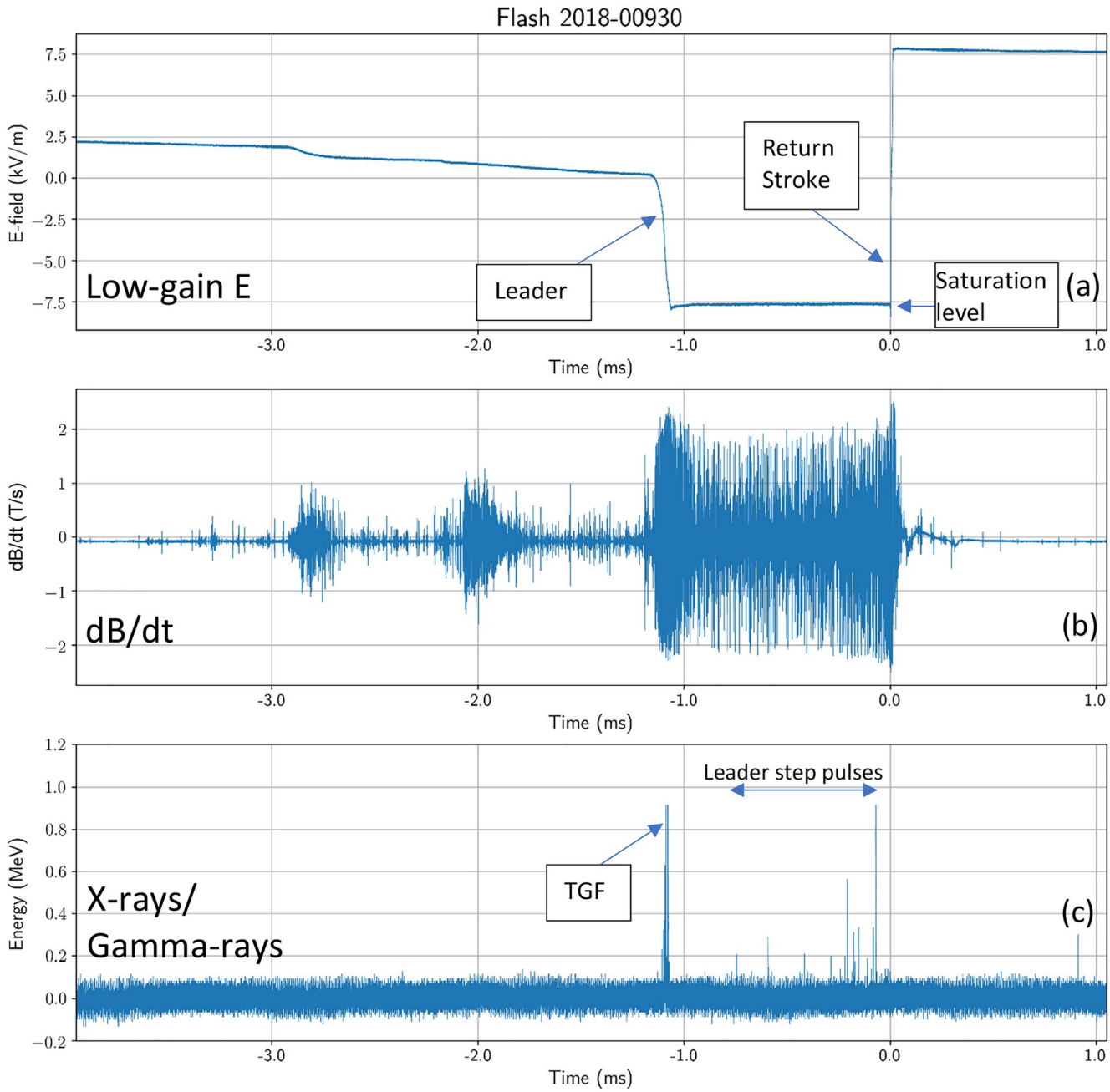

Figure 6. (a) Electric field waveform, (b) dB/dt waveform, and (c) X-rays/gamma-rays for Stroke 3 (negative). Terrestrial Gamma-ray Flash, marked in (c), is shown on an expanded time scale in Figure 7b. Time t = 0 corresponds to the onset of the return-stroke stage of Stroke 3. Note the different pulse-amplitude patterns for the Terrestrial Gamma-ray Flash and energetic radiation produced by leader steps in (c), while their maximum energy levels are about the same. Full time scale is 5 ms.

related to the relative age of the residual channels of Strokes 1 and 2) there. Additionally, there could be a local electric field enhancement inside the cloud associated with the abrupt change in the direction of leader propagation from predominantly horizontal to predominantly vertical (see Figure 6 and associated text). Clearly, further research is needed.

It is important to note that X-ray/gamma-ray pulses associated with leader stepping near ground are well known from many previous studies (e.g., Dwyer et al., 2004a; Mallick et al., 2012), while compact energetic radiation bursts characteristic of TGFs and occurring at the earlier (in-cloud) downward leader stage have never been reported before.

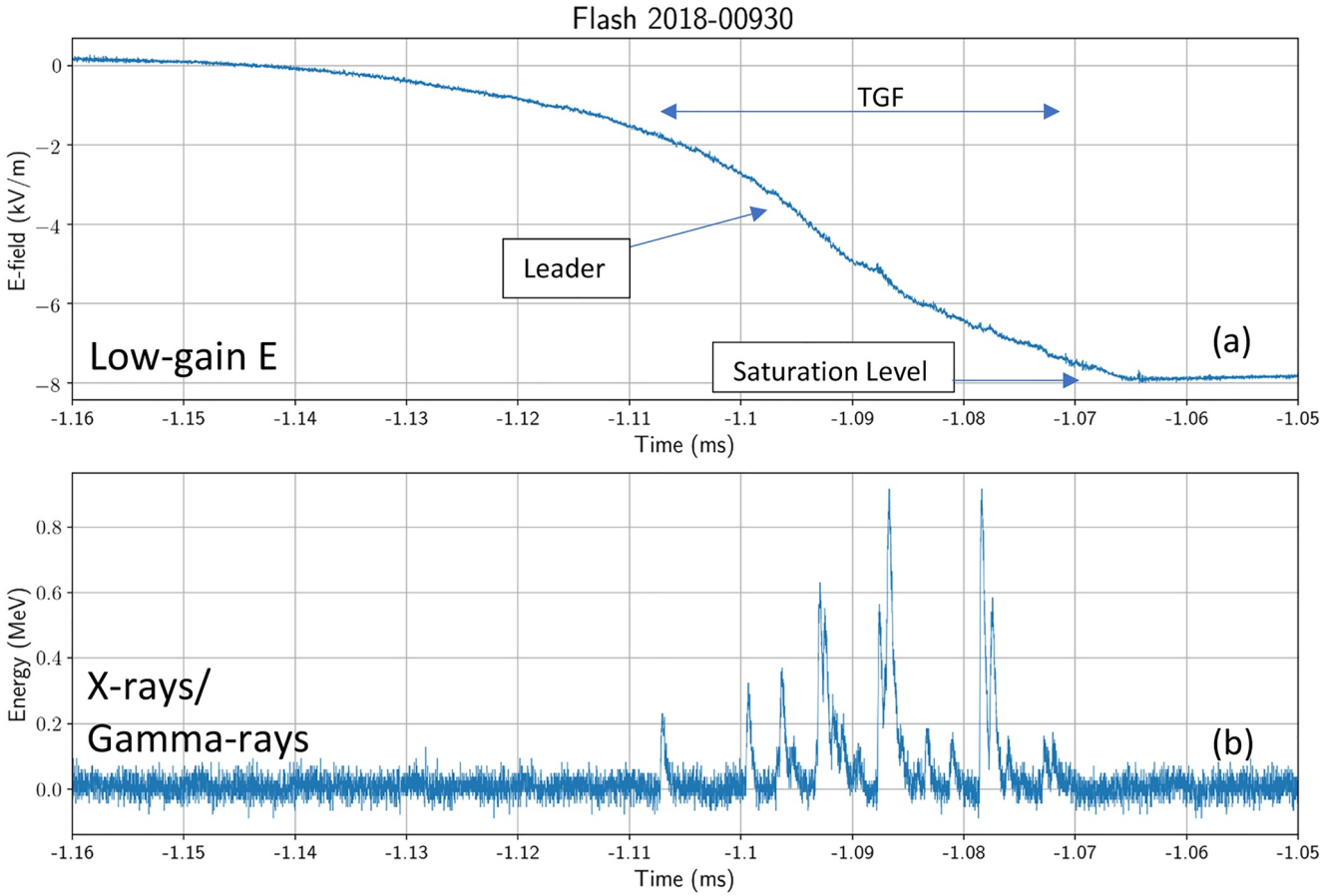

Figure 7. (a) Electric field waveform corresponding to the initial stage of the leader of Stroke 3 (negative). (b) Terrestrial Gamma-ray Flash associated with the in-cloud part of Stroke 3 leader entering the decayed channel to ground created by Stroke 2. Time t = 0 corresponds to the onset of the return-stroke stage of Stroke 3. Full time scale in is 110 μs. The corresponding dB/dt record is saturated.

3.5. Strokes 4 and 5 (Both Negative)

Stroke 4 created a new termination on ground, as evidenced by the NLDN-reported location shown in Figure 1, as well as by the leader duration between 10 and 15 ms, which is also indicative of a subsequent stroke forming a new ground termination (see Figure 4.14b of Rakov & Uman, 2003). Stroke 4 had an NLDN-reported peak current of 43 kA and contacted ground at a distance of 700 m from LOG. Electric field and dB/dt waveforms for this stroke are shown in Figures 8a and 8b, respectively. Stroke 4 produced no detectable X-rays, although Mallick et al. (2012) found that 100% of the strokes with peak currents between 40 and 60 kA produced detectable X-rays. In a follow-up study, Tran et al. (2019) concurrently analyzed the distance and peak-current dependence of X-ray emissions and found that the probability of a stroke with a peak current between 40 and 60 kA at a distance less than 1 km to produce detectable X-ray emission is 81%.

Like Stroke 4, Stroke 5 was negative. It apparently followed the same path to ground as Stroke 4, which was inferred from their overlapping location error ellipses (see Figure 1), as well as from the fact that Stroke 5 had relatively short leader duration estimated to be 1 ms or so (see Figure 9). We assign the more accurate (smaller NLDN location error ellipse) location of Stroke 4 to Stroke 5 and assume that they both occurred at a distance of 700 m from LOG. Stroke 5 had a relatively low NLDN-reported peak current (4.5 kA) and produced no detectable X-rays, which is consistent with relatively low probability of detection of X-ray emission from low-intensity strokes: 23% according to Tran et al. (2019).

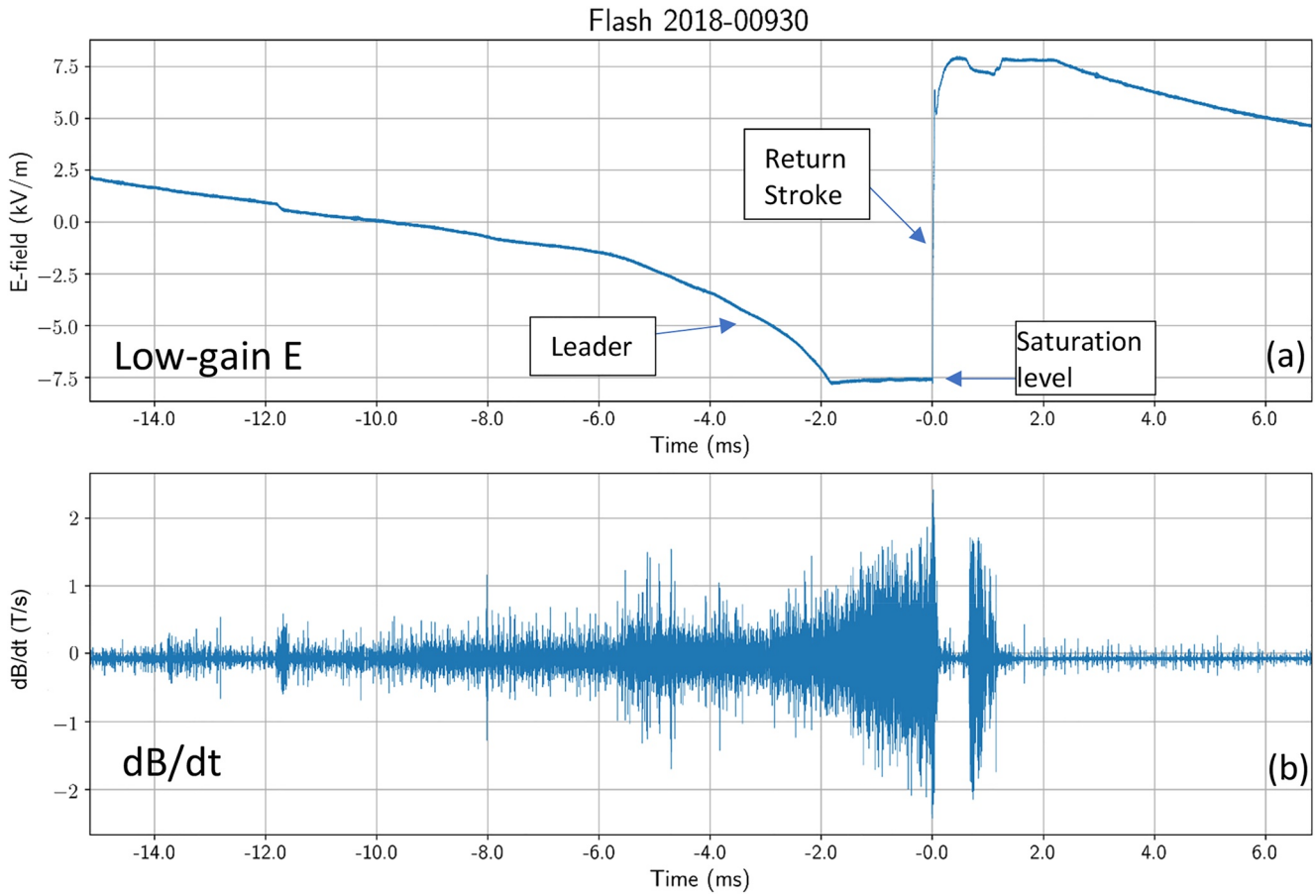

Figure 8. Same as Figure 5, but for Stroke 4 (negative). Time t = 0 corresponds to the onset of the return-stroke stage of Stroke 4. Full time scale is 22 ms.

4. Discussion and Concluding Remarks

TGFs previously observed at ground level in Florida (a total of four) were either associated with the initial continuous current (ICC) of rocket-triggered lightning flashes or occurred during the relatively steady current following the return-stroke current peak in natural lightning flashes; that is, in the presence of hot, current-carrying channel to ground, well after the flash initiation processes. In contrast, Belz et al. (2020), from recent ground-based observations at 1.4 km above sea level in Utah, reported TGFs associated with the preliminary breakdown (PB) process, when there was undisturbed (cold) air between the cloud base and ground. TGFs recorded at ground level during winter thunderstorms in Japan were reported by Wada, Enoto, Nakamura et al. (2019), (2020) and Hisadomi et al. (2021), who associated them with in-cloud processes producing -EIPs, as discussed in Section 1. It is presently not clear if some -EIPs are essentially the same as PB pulses (e.g., Lyu & Cummer, 2018), but in either case connection to ground does not exist.

Here, we reported on a TGF occurring in a context different from all previous observations, during a bipolar CG, with the gamma-ray emission being associated with the initial (in-cloud) phase of the negative leader presumably entering a less-decayed residual channel to ground near LOG. More specifically, the third (negative) stroke of the five-stroke bipolar flash produced the TGF as its leader, while developing in an older channel left behind by Stroke 1 inside the cloud (between roughly −3 and −1.2 ms; see Figure 6a), came in contact with the less-decayed and, hence, warmer channel to ground of the second (positive) stroke. It is also the first observation of TGF at ground level in the presence of a column of warm air (left behind by the

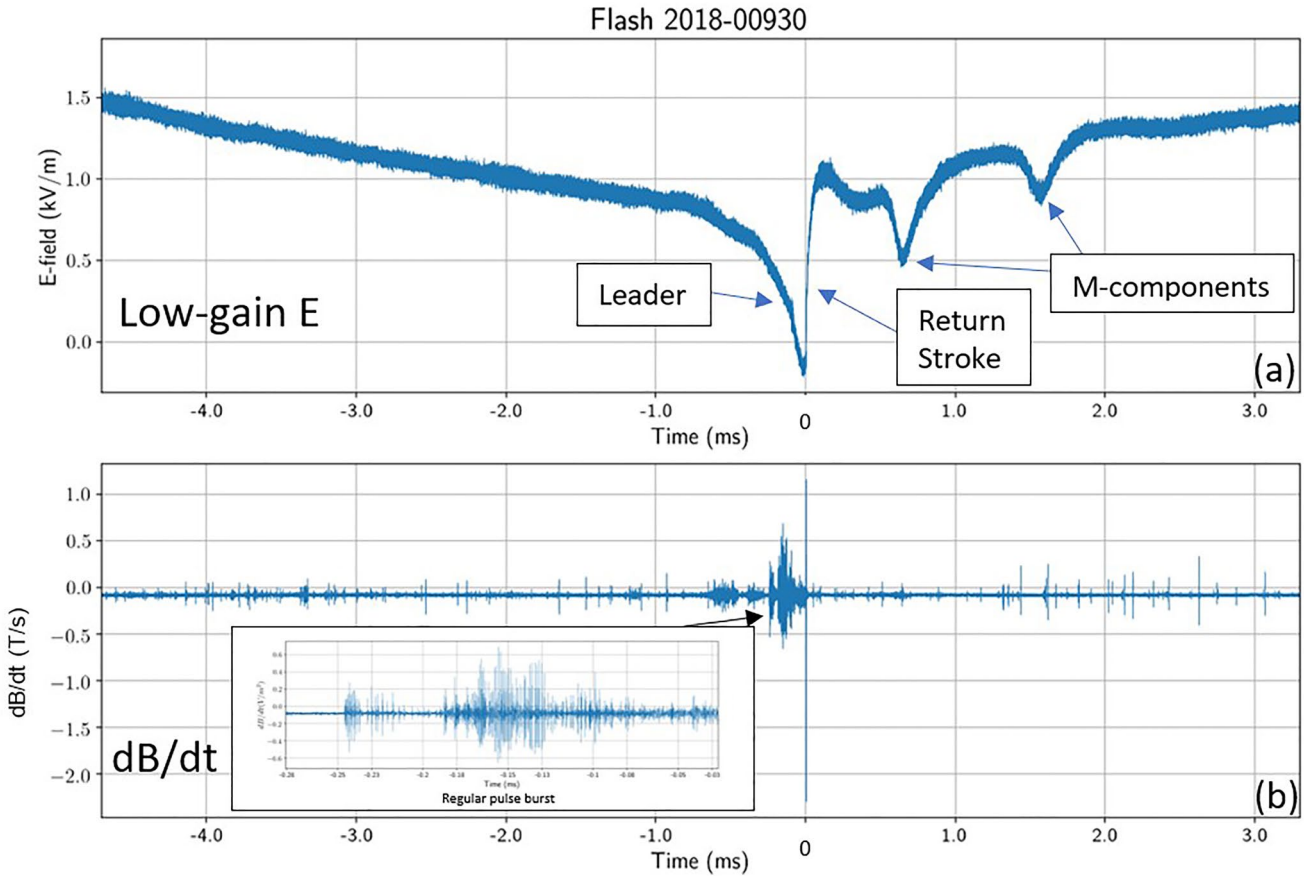

Figure 9. Same as Figure 5, but for Stroke 5 (negative). Time t = 0 corresponds to the onset of the return-stroke stage of Stroke 5. Full time scale is 8 ms. A regular pulse burst is shown in the inset in (b).

preceding stroke) between the cloud base and ground, as opposed to the presence of a hot grounded channel (all previous ground-based TGF observations in Florida) or no connection to ground at all (e.g., Belz et al., 2020). In addition, Stroke 1 and Stroke 3 (both negative) of this bipolar flash produced X-ray/gamma-ray emissions associated with leader steps. These X-ray/gamma-ray emission pulses produced near ground are clearly distinguishable in their overall pattern from the TGF that occurred during the initial (in-cloud) stage of the leader of Stroke 3.

Unlike the TGFs from Utah, which occurred during the flash-initiation process (i.e., when the air between the cloud base and ground was undisturbed), the subsequent-stroke leader producing the TGF presented in this paper encountered a warm (reduced air density) channel between the cloud base and ground, for which the friction curve is different from that for cold air (see Figure 10), and this may have had an impact on electron acceleration and avalanche formation process. As seen from the modified friction curve shown in red in Figure 10, at 3000 K (expected temperature of the decayed channel to be traversed by a subsequent leader; Uman & Voshall, 1968), the friction force, experienced by the electrons accelerated by the leader-tip electric field, is significantly reduced relative to cold (300 K) air in which first-stroke leaders have to propagate. Specifically, for cold air and E = 5 MV/m, only electrons with energy greater than 5 keV can run away, while for the air at 3000 K all electrons can do so. More favorable conditions for acceleration of electrons to runaway energies and formation of avalanches should be also encountered when the leader developing in an older (more decayed) channel enters a less-decayed channel. This is what likely happened when the leader of Stroke 3 entered the residual channel of Stroke 2, and this is when the compact burst of gamma-ray emission has occurred.

The role of reduced air density in reducing the breakdown electric field can also be explained in terms of the so-called reduced electric field defined as E/N, where E is the electric field in V/m and N is the air density in m^{-3}. The unit for the reduced breakdown electric field is Townsend (Td). The mean energy of electrons is typically a

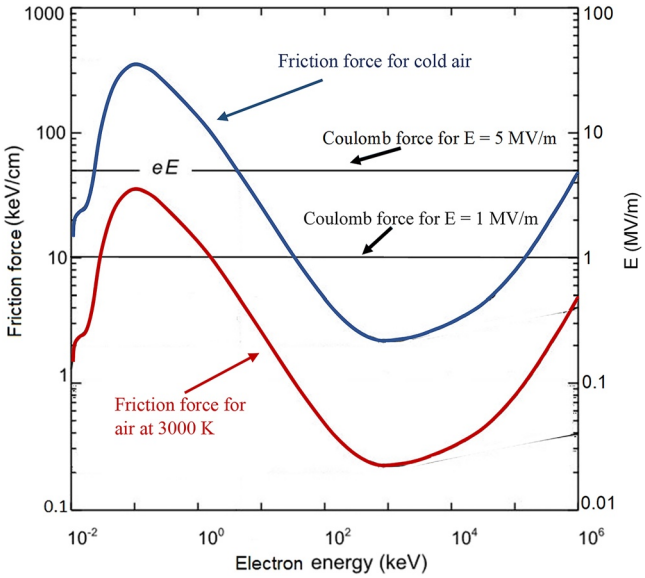

Figure 10. The dynamic friction curves showing the friction force (rate of energy loss per unit distance) experienced by an electron as a function of electron energy for cold air and for air at 3000 K. The curves include the effects of both inelastic scattering of the electron with air molecules and bremsstrahlung emission. The horizontal lines represent the Coulomb force acting on the electron (eE, where E is the electric field intensity and e is the electron charge) corresponding to E = 1 MV/m and E = 5 MV/m (see the right vertical scale). Electrons can run away to relativistic energies when the Coulomb force is greater than the friction force. For cold air and E = 5 MV/m, only electrons with energy greater than 5 keV can run away, while for the air at 3000 K all electrons can do so. Adapted from Dwyer (2004) and Tran et al. (2019).

function of E/N over a broad range of E and N. According to the concept of reduced electric field, lowering N by, say, a factor of 10 has the same consequences as increasing E by factor of 10.

Table 3 compares the various scenarios of acceleration and multiplication of runaway electrons in terms of the source of seed electrons, air temperature, and characteristic electric field. Conventional (non-relativistic) avalanches are additionally included as a reference. In Table 3, the ambient electron-energy distribution includes electrons with energies less than 30 eV or so, while the so-called cosmic-ray secondaries (electrons produced by very high energy (10^{15}–10^{16} eV or greater) cosmic-ray particles) have energies exceeding 0.1–1 MeV. For comparison, the average energy of electrons in conventional electric breakdown is just a few electron-volts. It follows from Table 3 that there are three main factors that can serve to initiate and sustain the multiplication of runaway electrons: (a) super-high electric field, (b) energetic electrons supplied by external sources, and (c) elevated air temperature (reduced air density). The present study provides additional support to the elevated-temperature scenario (previously considered by Mallick et al. (2012) and Tran et al. (2015), (2019)), which requires realistic (confirmed by modeling) electric fields and no energetic electrons from external sources. Further studies are needed to see if this scenario can quantitatively explain the ground-based observations of TGFs in Florida, as well as the occurrence of subsequent leaders generating more X-rays/gamma-rays near ground than their respective first leaders.

Note that the maximum energy of individual pulses in the TGF presented here (see Figure 7b) are between 0.9 and 1 MeV (with some influence of the piling-up effect); that is, near the border line between X-rays and gamma-rays, usually assumed in lightning research. In the present paper, we choose to classify this burst of energetic radiation as TGF, based on its duration (<1 ms), inferred location of its source inside the cloud, and the characteristic pulse occurrence pattern (compact burst), which is very different from that for the X-ray/gamma-ray pulses associated with leader stepping near ground (see Figure 6c and associated text). One possible explanation of the relatively low energies of the gamma rays observed in this study is not large enough voltage in front of the leader, so that the RREAs, seeded by energetic electrons from the warm channel, are not fully developed. Surely, this is just speculation, to be tested in future studies. It is worth noting that the TGF previously recorded with the same instrumentation at LOG (Tran et al., 2015) contained pulses exceeding the detector saturation level of 5–6 MeV with no evidence of the piling-up effect.

Ground-based observations of TGFs are rare, and there seems to be no single context in which they occur. It is becoming, however, clear (see Table 1 and discussion above) that the remnants of previously conditioned channels, necessarily present in the cloud during a multiple-stroke flash, can play an important role by creating relatively sharp air-density gradients in the clouds. Electric fields needed for the formation of runaway electron avalanches may be produced by leaders initially developing in cold air (before colliding with a warm channel) or by recoil leaders that are known to retrace decayed lightning channels or branches. Multiple branches at different

Table 3
Acceleration and Multiplication of Runaway Electrons

Process	Source of seed electrons	Air temperature, K	Electric field,[a] MV/m
Relativistic avalanches in cold air (cold runaway breakdown)	Two-step process starting with ambient distribution	300	≳30
Relativistic avalanches in cold air (RREA)	Cosmic-ray secondaries	300	~0.2
Relativistic avalanches in remnants of decayed channel	Ambient distribution	3,000	≳3
Conventional (non-relativistic) avalanches in cold air	Ambient distribution	300	~3

[a]Approximate values at sea level.

stages of development are likely to be present in the cloud during the relatively steady current flow to ground (as was the case in all previous ground-based observations of TGFs in Florida), some of those branches being at the decayed stage. The lack of observations of TGFs associated with the preliminary (initial) breakdown process in Florida could be related to the larger altitude of lightning initiation above the sea-level terrain in Florida compared to the 1.4-km elevated terrain in Utah and to low-altitude winter thunderclouds in Japan. It is not clear why no TGFs occurring well after the cloud-to-ground lightning initiation process; that is, when there exists a strong or weak (residual) electric connection to ground, were reported from the studies in Utah and Japan. Further research is needed to better understand the lightning processes giving rise to TGFs recorded at ground level.

Data Availability Statement

Figures were made with Matplotlib version 3.2.1 (Caswell et al., 2020; Hunter, 2007), available under the Matplotlib license at https://matplotlib.org/. The TGF data and electromagnetic field records (Kereszy et al., 2021) can be accessed at https://doi.org/10.5281/zenodo.5847090.

Acknowledgments
This research was supported in part by the U.S. National Science Foundation grant AGS-2114471. The authors would like to thank John Cramer and Vaisala for providing NLDN data. We would like to acknowledge Steve Prinzivalli, Jeff Lapierre, and Michael Stock of Earth Networks for useful discussions and for providing ENTLN data. Yanan Zhu wrote a code for plotting ENTLN data. Three anonymous reviewers provided useful comments on the paper.

References

Abbasi, R. U., Abu-Zayyad, T., Allen, M., Barcikowski, E., Belz, J. W., Bergman, D. R., et al. (2018). Gamma ray showers observed at ground level in coincidence with downward lightning leaders. *Journal of Geophysical Research: Atmospheres*, *123*(13), 6864–6879. https://doi.org/10.1029/2017JD027931

Baba, Y., & Rakov, V. A. (2007). Electromagnetic fields at the top of a tall building associated with nearby lightning return strokes. *IEEE Transactions on Electromagnetic Compatibility*, *49*(3), 632–643. https://doi.org/10.1029/2006JD007222

Belz, J. W., Krehbiel, P. R., Remington, J., Stanley, M. A., Abbasi, R. U., LeVon, R., et al. (2020). Observations of the origin of downward terrestrial gamma-ray flashes. *Journal of Geophysical Research: Atmospheres*, *125*(23). https://doi.org/10.1029/2019JD031940

Briggs, M. S., Fishman, G. J., Connaughton, V., Bhat, P. N., Paciesas, W. S., Preece, R. D., et al. (2010). First results on terrestrial gamma ray flashes from the fermi gamma-ray burst monitor. *Journal of Geophysical Research*, *115*(A7), A07323. https://doi.org/10.1029/2009JA015242

Caswell, T., Droettboom, M., Lee, A., Hunter, J., Firing, E., Stansby, D., et al. (2020). Matplotlib v3.2.1 [Software]. Zenodo. https://doi.org/10.5281/zenodo.3714460

Chilingarian, A., Khanikyants, Y., Mareev, E., Pokhsraryan, D., Rakov, V. A., & Soghomonyan, S. (2017). Types of lightning discharges that abruptly terminate enhanced fluxes of energetic radiation and particles observed at ground level. *Journal of Geophysical Research: Atmospheres*, *122*(14), 7582–7599. https://doi.org/10.1002/2017JD026744

Chilingarian, A., Khanikyants, Y., Rakov, V. A., & Soghomonyan, S. (2020). Termination of thunderstorm-related bursts of energetic radiation and particles by inverted intracloud and hybrid lightning discharges. *Atmospheric Research*, *223*, 104713. https://doi.org/10.1016/j.atmosres.2019.104713

Dwyer, J. R. (2004). Implications of x-ray emission from lightning. *Geophysical Research Letters*, *31*(12), L12102. https://doi.org/10.1029/2004GL019795

Dwyer, J. R., Rassoul, H. K., Al-Dayeh, M., Caraway, L., Wright, B., Chrest, A., et al. (2004b). A ground level gamma-ray burst observed in association with rocket-triggered lightning. *Geophysical Research Letters*, *31*(5), L05119. https://doi.org/10.1029/2003GL018771

Dwyer, J. R., Rassoul, H. K., Al-Dayeh, M., Caraway, L., Wright, B., Chrest, A., et al. (2004a). Measurements of X-ray emission from rocket-triggered lightning. *Geophysical Research Letters*, *31*(5), L05118. https://doi.org/10.1029/2003GL018770

Dwyer, J. R., Schaal, M. M., Cramer, E., Arabshahi, S., Liu, N., Rassoul, H. K., et al. (2012). Observation of a gamma-ray flash at ground level in association with a cloud-to-ground lightning return stroke. *Journal of Geophysical Research*, *117*(A10), A10303. https://doi.org/10.1029/2012JA017810

Dwyer, J. R., Uman, M. A., Rassoul, H. K., Al-Dayeh, M., Caraway, L., Jerauld, J., et al. (2003). Energetic radiation produced during rocket-triggered lightning. *Science*, *299*(5607), 694–697. https://doi.org/10.1126/science.1078940

Fishman, G. J., Bhat, P. N., Mallozzi, R., Horack, J. M., Koshut, T., Kouveliotou, C., et al. (1994). Discovery of intense gamma-ray flashes of atmospheric origin. *Science*, *264*(5163), 1313–1316. https://doi.org/10.1126/science.264.5163.1313

Hare, B. M., Uman, M. A., Dwyer, J. R., Jordan, D. M., Biggerstaff, M. I., Caicedo, J. A., et al. (2016). Ground-level observation of a terrestrial gamma-ray flash initiated by a triggered lightning. *Journal of Geophysical Research: Atmospheres*, *121*(11), 6511–6533. https://doi.org/10.1002/2015JD024426

Hisadomi, S., Nakazawa, K., Wada, Y., Tsuji, Y., Enoto, T., Shinoda, T., et al. (2021). Multiple gamma-ray glows and a downward TGF observed from nearby thunderclouds. *Journal of Geophysical Research: Atmospheres*, *126*(18), e2021JD034543. https://doi.org/10.1029/2021JD034543

Hunter, J. D. (2007). Matplotlib: A 2D graphics environment. *Computing in Science & Engineering*, *9*(3), 90–95. https://doi.org/10.1109/MCSE.2007.55

Kereszy, I., Rakov, V. A., Ding, Z., & Dwyer, J. R. (2021). TGF data and electromagnetic field records. [Dataset]. Zenodo. https://doi.org/10.5281/zenodo.5847090

Lyu, F., & Cummer, S. A. (2018). Energetic radio emissions and possible terrestrial gamma-ray flashes associated with downward propagating negative leaders. *Geophysical Research Letters*, *45*(19), 10764–10771. https://doi.org/10.1029/2018GL079424

Lyu, F., Cummer, S. A., & McTague, L. (2015). Insights into high peak current in-cloud lightning events during thunderstorms. *Geophysical Research Letters*, *42*(16), 6836–6843. https://doi.org/10.1002/2015GL065047

Mallick, S., Rakov, V. A., & Dwyer, J. R. (2012). A study of X-ray emissions from thunderstorms with emphasis on subsequent strokes in natural lightning. *Journal of Geophysical Research*, *117*(D16), D16107. https://doi.org/10.1029/2012JD017555

McClave, J. T., & Dietrich, F. H. (1979). *Statistics*. Dellen Publishing Company.

Nag, A., & Rakov, V. A. (2016). A unified engineering model of the first stroke in downward negative lightning. *Journal of Geophysical Research: Atmospheres*, *121*(5), 2188–2204. https://doi.org/10.1002/2015JD023777

Neubert, T., Ostgaard, N., Reglero, V., Chanrion, O., Heumesser, M., Dimitriadou, K., et al. (2020). Terrestrial gamma-ray flashes and ionospheric UV emissions generated by lightning. *Science*, *367*(6474), 183–186. https://doi.org/10.1126/science.aax3872

Østgaard, N., Cummer, S. A., Mezentsev, A., Luque, A., Dwyer, J., Neubert, T., et al. (2021). Simultaneous observations of EIP, TGF, Elve, and optical lightning. *Journal of Geophysical Research: Atmospheres*, *126*(11), e2020JD033921. https://doi.org/10.1029/2020JD033921

Rakov, V. A. (2005). *Lightning flashes transporting both negative and positive charges to ground*. In C., Pontikis (Ed.), *Recent Progresses in Lightning Physics* (pp. 9–21). Research Signpost.

Rakov, V. A., & Uman, M. A. (2003). *Lightning:Physics and effects*. Cambridge University Press.

Saba, M. M. F., Schumann, C., Warner, T. A., Helsdon, J. H., Schulz, W., & Orville, R. E. (2013). Bipolar cloud-to-ground lightning flash observations. *Journal of Geophysical Research: Atmospheres*, *118*(19), 11098–11106. https://doi.org/10.1002/jgrd.50804

Saraiva, A. C. V., Campos, L. Z. S., Williams, E. R., Zepka, G. S., Alves, J., Pinto, O., et al. (2014). High-speed video and electromagnetic analysis of two natural bipolar cloud-to-ground lightning flashes. *Journal of Geophysical Research: Atmospheres*, *119*(10), 6105–6127. https://doi.org/10.1002/2013JD020974

Smith, D. M., Lopez, L. I., Lin, R. P., & Barrington-Leigh, C. P. (2005). Terrestrial gamma-ray flashes observed up to 20 MeV. *Science*, *307*(5712), 1085–1088. https://doi.org/10.1126/science.1107466

Tilles, J. N., Krehbiel, P. R., Stanley, M. A., Rison, W., Liu, N., Lyu, F., et al. (2020). Radio interferometer observations of an energetic in-cloud pulse reveal large currents generated by relativistic discharges. *Journal of Geophysical Research: Atmospheres*, *125*(20), e2020JD032603. https://doi.org/10.1029/2020JD032603

Tran, M. D., Kereszy, I., Rakov, V. A., & Dwyer, J. R. (2019). On the role of reduced air density along the lightning leader path to ground in increasing X-ray production relative to normal atmospheric conditions. *Geophysical Research Letters*, *46*(15), 9252–9260. https://doi.org/10.1029/2019GL083753

Tran, M. D., Rakov, V., Mallick, S., Dwyer, J., Nag, A., & Heckman, S. (2015). A terrestrial gamma-ray flash recorded at the Lightning Observatory in Gainesville, Florida. *Journal of Atmospheric and Solar-Terrestrial Physics*, *136*(A), 86–93. https://doi.org/10.1016/j.jastp.2015.10.010

Uman, M. A., & Voshall, R. E. (1968). Time interval between lightning strokes and the initiation of dart leaders. *Journal of Geophysical Research*, *73*(2), 497–506. https://doi.org/10.1029/JB073i002p00497

Wada, Y., Enoto, T., Nakamura, Y., Furuta, Y., Yuasa, T., Nakazawa, K., et al. (2019). Gamma-ray glow preceding downward terrestrial gamma-ray flash. *Communications on Physics*, *2*(1), 67. https://doi.org/10.1038/s42005-019-0168-y

Wada, Y., Enoto, T., Nakazawa, K., Furuta, Y., Yuasa, T., Nakamura, Y., et al. (2019). Downward terrestrial gamma-ray flash observed in a winter thunderstorm. *Physical Review Letters*, *123*(6), 061103. https://doi.org/10.1103/PhysRevLett.123.061103

Wada, Y., Enoto, T., Nakamura, Y., Morimoto, T., Sato, M., Ushio, T., et al. (2020). High peak-current lightning discharges associated with downward terrestrial gamma-ray flashes. *Journal of Geophysical Research: Atmospheres*, *125*(4), e2019JD031730. https://doi.org/10.1029/2019JD031730

Zhu, Y., Rakov, V. A., & Tran, M. D. (2016). A study of preliminary breakdown and return stroke processes in high-intensity negative lightning discharges, Atmosphere, Special Issue. *Electromagnetic Fields and Waves with Special Attention to Lightning Flashes*, *7*(10), 130. https://doi.org/10.3390/atmos7100130